J|A|C|S
ARTICLES
Published on Web 12/20/2006

Electrochemical Investigations of the Interconversions between Catalytic and Inhibited States of the [FeFe]-Hydrogenase from *Desulfovibrio desulfuricans*

Alison Parkin,[†] Christine Cavazza,[‡] Juan C. Fontecilla-Camps,*[,‡] and Fraser A. Armstrong*[,†]

Contribution from the Inorganic Chemistry Laboratory, Department of Chemistry, Oxford University, South Parks Road, Oxford OX1 3QR, England, and Laboratoire de Cristallographie et de Cristallogènese de Protéines, Institut de Biologie Structurale JP Ebel (CEA-CNRS-UJF), 41 rue Jules Horowitz, 38027 Grenoble Cédex 1, France

Received June 22, 2006; E-mail: fraser.armstrong@chem.ox.ac.uk; juan.fontecilla@ibs.fr

Abstract: Studies of the catalytic properties of the [FeFe]-hydrogenase from *Desulfovibrio desulfuricans* by protein film voltammetry, under a H_2 atmosphere, reveal and establish a variety of interesting properties not observed or measured quantitatively with other techniques. The catalytic bias (inherent ability to oxidize hydrogen vs reduce protons) is quantified over a wide pH range: the enzyme is proficient at both H_2 oxidation (from pH > 6) and H_2 production (pH < 6). Hydrogen production is inhibited by H_2, but the effect is much smaller than observed for [NiFe]-hydrogenases from *Allochromatium vinosum* or *Desulfovibrio fructosovorans*. Under anaerobic conditions and positive potentials, the [FeFe]-hydrogenase is oxidized to an inactive form, inert toward reaction with CO and O_2, that rapidly reactivates upon one-electron reduction under 1 bar of H_2. The potential dependence of this interconversion shows that the oxidized inactive form exists in two pH-interconvertible states with $pK_{ox} = 5.9$. Studies of the CO-inhibited enzyme under H_2 reveals a strong enhancement of the rate of activation by white light at −109 mV (monitoring H_2 oxidation) that is absent at low potential (−540 mV, monitoring H^+ reduction), thus demonstrating photolability that is dependent upon the oxidation state.

Introduction

Hydrogenases are microbial metalloenzymes which catalyze the interconversion between H_2 and protons and electrons (eq 1). The two main classes are known as [FeFe]-hydrogenases

$$H_2 \leftrightarrow 2H^+ + 2e^- \quad (1)$$

and [NiFe]-hydrogenases. Enzymes from both classes usually react rapidly with O_2 and CO, which are potent inhibitors.[1−6] Consequently, overcoming inhibition or permanent damage is a challenge for microbes, as well as for future technologies aiming to exploit or mimic these catalysts for electrochemical hydrogen cycling or improve them for biological H_2 production.[7−10] In previous papers we have described experiments that have helped unravel the complex chemistry of [NiFe]-hydrogenases.[3,11−18] In this paper we focus on a representative [FeFe]-hydrogenase, the enzyme from *Desulfovibrio desulfuricans* (*Dd* hydrogenase), and seek to identify and measure factors that influence and control its catalytic activity.

Two [FeFe]-hydrogenase crystal structures have been solved, that of the enzyme from *Dd* (Figure 1) and hydrogenase I from *Clostridium pasteurianum* (*Cp* I).[19,20] The two hydrogenases

[†] Oxford University.
[‡] Institut de Biologie Structurale JP Ebel (CEA-CNRS-UJF).

(1) Vincent, K. A.; Parkin, A.; Lenz, O.; Albracht, S. P. J.; Fontecilla-Camps, J. C.; Cammack, R.; Friedrich, B.; Armstrong, F. A. *J. Am. Chem. Soc.* **2005**, *127*, 18179−18189.
(2) Léger, C.; Dementin, S.; Bertrand, P.; Rousset, M.; Guigliarelli, B. *J. Am. Chem. Soc.* **2004**, *126*, 12162−12172.
(3) Lamle, S. E.; Vincent, K. A.; Halliwell, L. M.; Albracht, S. P. J.; Armstrong, F. A. *Dalton Trans.* **2003**, *21*, 4152−4415.
(4) Ogata, H.; Mizoguchi, Y.; Mizuno, N.; Miki, K.; Adachi, S.; Yasuoka, N.; Yagi, T.; Yamauchi, O.; Hirota, S.; Higuchi, Y. *J. Am. Chem. Soc.* **2002**, *124*, 11628−11635.
(5) Adams, M. W. W. *Biochim. Biophys. Acta* **1990**, *1020*, 115−145.
(6) Cammack, R.; Patil, D. S.; Hatchikian, E. C.; Fernàndez, V. M. *Biochim. Biophys. Acta* **1987**, *912*, 98−109.
(7) Tard, C.; Liu, X.; Ibrahim, S. K.; Bruschi, M.; Gioia, L. D.; Davies, S. C.; Yang, X.; Wang, L.-S.; Sawers, G.; Pickett, C. J. *Nature* **2005**, *433*, 610−613.
(8) Ghirardi, M. L.; King, P. W.; Posewitz, M. C.; Maness, P. C.; Fedorov, A.; Kim, K.; Cohen, J.; Schulten, K.; Seibert, M. *Biochem. Soc. Trans.* **2005**, *33*, 102−104.
(9) Mertens, R.; Liese, A. *Curr. Opin. Biotechnol.* **2004**, *15*, 343−348.
(10) Happe, T.; Hemschemeier, A.; Winkler, M.; Kaminski, A. *Trends Plant Sci.* **2002**, *7*, 246−250.
(11) Vincent, K. A.; Belsey, N. A.; Lubitz, W.; Armstrong, F. A. *J. Am. Chem. Soc.* **2006**, *128*, 7448−7449.
(12) Lamle, S. E.; Albracht, S. P. J.; Armstrong, F. A. *J. Am. Chem. Soc.* **2005**, *127*, 6595−6604.
(13) Lamle, S. E.; Albracht, S. P. J.; Armstrong, F. A. *J. Am. Chem. Soc.* **2004**, *126*, 14899−14909.
(14) Jones, A. K.; Lamle, S. E.; Pershad, H. R.; Vincent, K. A.; Albracht, S. P. J.; Armstrong, F. A. *J. Am. Chem. Soc.* **2003**, *125*, 8505−8514.
(15) Jones, A. K.; Sillery, E.; Albracht, S. P. J.; Armstrong, F. A. *Chem. Commun.* **2002**, 866−867.
(16) Léger, C.; Jones, A. K.; Albracht, S. P. J.; Armstrong, F. A. *J. Phys. Chem. B* **2002**, *106*, 13058−13063.
(17) Léger, C.; Jones, A. K.; Roseboom, W.; Albracht, S. P. J.; Armstrong, F. A. *Biochemistry* **2002**, *41*, 15736−15746.
(18) Pershad, H. R.; Duff, J. L. C.; Heering, H. A.; Duin, E. C.; Albracht, S. P. J.; Armstrong, F. A. *Biochemistry* **1999**, *38*, 8992−8999.
(19) Nicolet, Y.; Piras, C.; Legrand, P.; Hatchikian, C. E.; Fontecilla-Camps, J. C. *Structure* **1999**, *7*, 13−23.

10.1021/ja064425i CCC: $33.50

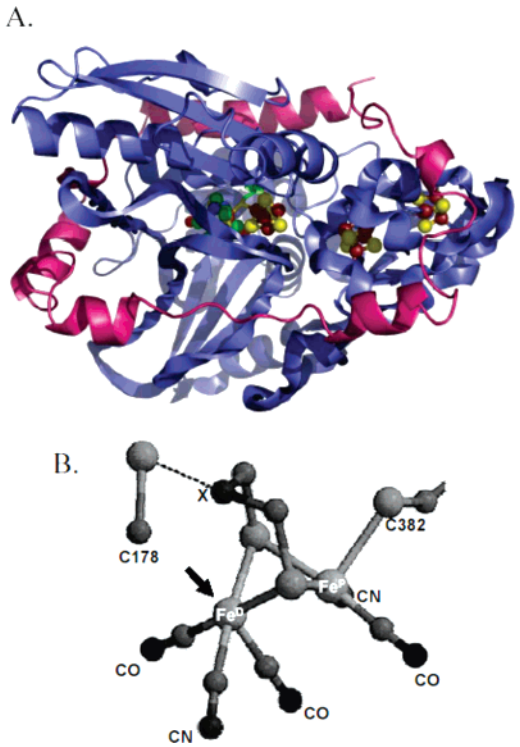

Figure 1. (A) Structure of *Dd* [FeFe]-hydrogenase (PDB code 1HFE).[19] The large subunit is shown in blue and the small subunit is shown in magenta, with [4Fe−4S] clusters and the active site marked as colored spheres. (B) Active site of a reduced form.[21] The Fe atom on the right is defined as the proximal Fe (relative to the neighboring [Fe−S] cluster), Fe^P; the Fe atom on the left is defined as the distal Fe, Fe^D. The arrow indicates the potential hydron binding site on Fe^D that is occupied by either H_2O or an extrinsic CO in the structure of *Cp* I.[20,23] Also shown is a close contact between the bridgehead atom X of the exogenous dithiolate ligand and the S atom of cysteine-178.

share common features, one being that the binuclear active site is buried but electronically connected to the surface by a series of [4Fe−4S] clusters. The active-site Fe atoms are each coordinated by one CO and one CN^- ligand, and the proximal Fe (Fe^P) is bound to the protein by a cysteine S that is bridged to a [4Fe−4S] cluster. The two Fe atoms are bridged by both sulfurs of an unusual organic 1,3-dithiolate ligand, and there is also a terminal CO on Fe^D that changes to bridging as a function of the redox state of the enzyme.[21] In addition, *Cp* I contains a H_2O bound to Fe^D that was not reported for *Dd*.[22]

The nature of the bridgehead atom (C, N, or O) in the 1,3-dithiolate ligand could not be explicitly elucidated from the X-ray data on *Dd* hydrogenase crystals[19] and is therefore shown as X in Figure 1B. The bridging ligand is postulated to be a bis(thiomethyl)amine on the basis of mechanistic considerations,[21] and this is supported by models[24] and by the short distance (3.1 Å) between the S-atom of C178 and atom X, which suggests a hydrogen bond.

The amino acid sequence of the [FeFe]-hydrogenase from *Dd* is identical to its counterpart in *Desulfovibrio vulgaris* Hildenborough[25] (*Dv*) which has been extensively studied by spectroscopy.[26−32] The binuclear center in both enzymes has been identified in three oxidation states: H_{red}, H_{ox}, and H_{ox}^{inact}.[26,33−35] Aerobic purification of *Dd* and *Dv* hydrogenases yields the H_{ox}^{inact} state, which is postulated to be 1 electron more oxidized than H_{ox} (but see below) and resistant to damage by O_2.[28,35,36] Reductive activation under H_2 yields the H_{red} and H_{ox} states, which are irreversibly inactivated by O_2. Anaerobic reoxidation of the H_2-reduced *Dv* enzyme reconverts it to the O_2-stable H_{ox}^{inact} state.[37] Exogenous CO reversibly inhibits [FeFe]-hydrogenases,[5,23,33,34,38] and crystallographic studies on *Cp* I have shown that CO binds to the Fe^D site facing the channel.[23] At low temperatures, the EPR signal of the CO-inhibited enzyme is reversibly converted by light into the rhombic "$g = 2.10$" signal characteristic of the active H_{ox} state.[27] The CO-inhibited form is thus assigned as H_{ox}−CO.[33]

Controversy exists over the precise assignment of Fe oxidation states in the H_{red}, H_{ox}, and H_{ox}^{inact} forms of [FeFe]-hydrogenases.[28,39] In considering this issue, the linked [4Fe−4S] cluster must also be taken into account as a potential site for an electron, although no stable form of $[4Fe-4S]^+$ has been positively identified.[39] A further complication is that the true oxidation level of the active site is also determined by the presence or absence of the substrate, H_2 or H^- (hydride): active-site states differing by *two electrons* "belonging" to hydrogen ligands may therefore not be distinguished easily or at all by EPR or X-ray diffraction. The active site is EPR-silent in the H_{red} state, but H_{ox}, believed to be 1 electron more oxidized than H_{red}, is EPR-active with $g = 2.10$, 2.04, 2.00 (the $g = 2.10$ signal). The unpaired spin on H_{ox} dictates its formal assignment as either Fe(I)−Fe(II) or Fe(II)−Fe(III). Discussions in this paper are based on the assumption that for H_{ox} the binuclear center corresponds to Fe(I)−Fe(II) with possible delocalization onto the [4Fe−4S] cluster. We make this assumption because H_{ox}^{inact} is highly unlikely to be Fe(III)−Fe(III) as coordination of Fe(III) by CO and *hydrogen-bonded* π-accepting CN^- ligands will not be favored.

Here we have used protein film voltammetry (PFV) to investigate reactions of the [FeFe]-hydrogenase from *Dd* and obtain new information on the interconversions between dif-

(20) Peters, J. W.; Lanzilotta, W. N.; Lemon, B. J.; Seefeldt, L. C. *Science* **1998**, *282*, 1853−1858.
(21) Nicolet, Y.; de Lacey, A. L.; Vernede, X.; Fernàndez, V. M.; Hatchikian, E. C.; Fontecilla-Camps, J. C. *J. Am. Chem. Soc.* **2001**, *123*, 1596−1601.
(22) Nicolet, Y.; Lemon, B. J.; Fontecilla-Camps, J. C.; Peters, J. W. *Trends Biochem. Sci.* **2000**, *25*, 138−143.
(23) Lemon, B. J.; Peters, J. W. *Biochemistry* **1999**, *38*, 12969−12973.
(24) Henry, R. M.; Shoemaker, R. K.; DuBois, D. L.; DuBois, M. R. *J. Am. Chem. Soc.* **2006**, *128*, 3002−3010.
(25) Hatchikian, E. C.; Magro, V.; Forget, N.; Nicolet, Y.; Fontecilla-Camps, J. C. *J. Bacteriol.* **1999**, *181*, 2947−2952.
(26) Patil, D. S.; Moura, J. G.; He, S. H.; Teixeira, M.; Prickril, B. C.; DerVartanian, D. V.; Peck, H. D., Jr.; LeGall, J.; Huynh, B.-H. *J. Biol. Chem.* **1988**, *263*, 18732−18738.
(27) Patil, D. S.; Huynh, B. H. *J. Am. Chem. Soc.* **1988**, *110*, 8533−8534.
(28) Pereira, A. S.; Tavares, P.; Moura, I.; Moura, J. J. G.; Huynh, B. H. *J. Am. Chem. Soc.* **2001**, *123*, 2771−2782.
(29) Patil, D. S.; He, S. H.; DerVartanian, D. V.; Gall, J. L.; Huynh, B. H.; Peck, H. D., Jr. *FEBS Lett.* **1988**, *228*, 85−88.
(30) Hagen, E. R.; van Berkel-Arts, A.; Kruse-Wolters, K.; Dunham, W. R.; Veeger, C. *FEBS Lett.* **1986**, *201*, 158−162.
(31) Huynh, B. H.; Czechowski, M. H.; Kruger, H.-J.; DerVartanian, D. V.; Peck, H. D., Jr.; LeGall, J. *Proc. Natl. Acad. Sci. U.S.A.* **1984**, *81*, 3728−3732.
(32) Pierik, A.; Hulstein, M.; Hagen, W.; Albracht, S. *Eur. J. Biochem.* **1998**, *258*, 572−578.
(33) Albracht, S. P. J.; Roseboom, W.; Hatchikian, E. C. *J. Biol. Inorg. Chem.* **2006**, *11*, 88−101.
(34) Roseboom, W.; de Lacey, A. L.; Fernàndez, V. M.; Hatchikian, E. C.; Albracht, S. P. J. *J. Biol. Inorg. Chem.* **2006**, *11*, 102 - 118.
(35) Hatchikian, E. C.; Forget, N.; Fernàndez, V. M.; Williams, R.; Cammack, R. *Eur. J. Biochem.* **1992**, *209*, 357−365.
(36) van der Westen, H. M.; Mayhew, S. G.; Veeger, C. *FEBS Lett.* **1978**, *86*, 122−126.
(37) van Dijk, C.; van Berkel-Arts, A.; Veeger, C. *FEBS Lett.* **1983**, *156*, 340−344.
(38) Thauer, R. K.; Kaufer, B.; Zahringer, M.; Jungermann, K. *Eur. J. Biochem.* **1974**, *42*, 447−452.
(39) Popescu, C. V.; Münck, E. *J. Am. Chem. Soc.* **1999**, *121*, 7877−7884.

ferent states. Protein film voltammetry refers to a suite of electrochemical techniques that address the redox chemistry of enzymes immobilized on electrodes.[17,40,41] Electron transfer and chemical processes that otherwise appear entangled are easily observed and resolved in both potential and time domains. The information from PFV focuses on *turnover* conditions, *under* H_2, with the high inherent activity greatly amplifying the electrochemical signals.

Materials and Methods

The enzyme was purified as described previously,[35] except that fully anaerobic conditions were used throughout. The all-glass electrochemical cell was clamped tightly to an all-glass head fitting precisely around the electrode rotator (EG&G M636), thus sealing the internal headspace (volume 200 mL) of the cell from the glovebox atmosphere.[40] This design allowed gases to be introduced and evacuated quickly and reliably at a constant pressure through inlet and outlet side arms, and less than 5 min was required to achieve complete equilibration with the cell solution when the electrode was rotated at 2500 rpm (this rotation rate was used throughout, as it was sufficiently fast to remove substrate mass-transport effects). The rotating disk pyrolytic graphite "edge" (PGE) electrode[42] was polished with an aqueous alumina slurry (1 μm Al_2O_3, Buehler) and sonicated thoroughly before each experiment. The counter electrode was a platinum wire, and the saturated calomel reference electrode (SCE) was situated in a Luggin side arm filled with 0.1 M NaCl. The main cell compartment was jacketed and thermostated, and the reference electrode side arm was well separated and kept at 25 $\pm$ 1 °C (a nonisothermal configuration). Both the head and cell were encased in black tape to ensure that light was excluded, thus avoiding any possible photolytic reactions.[5,23,27,33,34,38,43,44] For experiments in which the electrode was illuminated, the tape at the bottom of the cell was removed to allow exposure to light from a battery-powered halogen lamp (10 W, 6 V, with 7 cm separation between the base of the light bulb and the tip of the electrode). The power output of this setup was 20 mW cm^{-2}, and it was determined that there was no heating effect on the cell solution. The reference potential was corrected with respect to the standard hydrogen electrode (SHE) using $E_{SHE} = E_{SCE} + 242$ mV at 25 °C, and all values were adjusted to conform to the SHE scale. Experiments were performed using an Autolab PGSTAT 10 electrochemical analyzer with GPES software (Eco Chemie, The Netherlands). For the potential-step experiments, the current was sampled at least every second following the step (duration $<<1$ s).

A mixed buffer system[14] was used in all experiments, and unless stated otherwise this also contained 200 μg/mL polymyxin-B sulfate, which acts as a stabilizing coadsorbate.[17] Concentrations of O_2 and CO were estimated assuming the concentration in the stock solution injected into the cell was that expected for equilibrium with 1 bar of gas at room temperature, i.e., approximately 1 mM.

For each experiment, a film of *Dd* hydrogenase was formed by immersing a freshly polished electrode in a "forming" solution consisting of 15 μL of enzyme solution (85 μM), 10 μL of 20 mg mL^{-1} polymyxin-B sulfate, and 975 μL of pH 6.0 buffer (final enzyme concentration approximately 1.2 μM). The potential was held at -558 mV, resulting in a H^+ reduction current that increased to a limiting value as hydrogenase adsorbed on the electrode. Cyclic voltammetry without enzyme showed no currents due to H_2 oxidation or H^+ reduction over the range $+400$ to -650 mV. For all experiments, the cell was maintained at 10 °C to minimize loss of enzyme activity on the electrode, from either desorption or other potential-independent inactivation. At 10 °C this loss was sufficiently slow to pose few complications.

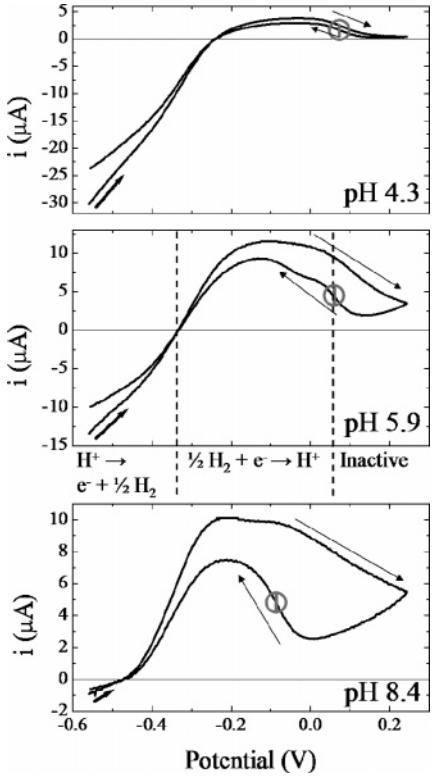

Figure 2. How the bidirectional activity of *Dd* [FeFe]-hydrogenase varies with pH. Conditions: 1 bar of H_2, electrode rotation rate 2500 rpm, scan rate 10 mV s^{-1}, temperature 10 °C. Black arrows indicate the direction of cycling, and circled vertical gray lines indicate the positions of E_{switch}. Dashed lines on the 10 mV s^{-1}, pH 5.9 voltammogram partition the scan according to three different potential regions: H^+ reduction, H_2 oxidation, and anaerobic inactivation.

Results and Discussion

A. Under H_2, Three Potential Regions Define H_2 Production, H_2 Oxidation, and the Existence of an Inactive "Resting" State. Figure 2 shows cyclic voltammograms measured on the same film. The pH 4.3 scan was measured first, after the film had equilibrated with pH 4.3 buffer. The H^+ concentration was adjusted to pH 5.9 by injecting 0.1 mL of 0.47 M NaOH and then to pH 8.4 by injecting a further 0.2 mL of 0.47 M NaOH. The voltammograms can be separated into three main regions—"H^+ reduction", "H_2 oxidation", and "(anaerobic) inactive" (or "resting")—as annotated for the pH 5.9 cycle. At low potential a negative current is observed, corresponding to the catalytic reduction of H^+. As the electrode potential is swept in the positive direction, the rate of H^+ reduction decreases, and eventually a positive current due to catalytic H_2 oxidation is observed. The intersection of current with the *x*-axis (the zero current potential) is the $2H^+/H_2$ reversible electrode potential for that particular pH (and thus an internal pH reference). At even higher potential, the current drops, ultimately to zero if sufficient time is allowed. We refer to the inactivation at high potential as a "switch-off". Upon reversal of the scan direction, a corresponding sigmoidal rise in current is observed, i.e., a "switch-on". These processes are discussed in detail later.

(40) Vincent, K. A.; Armstrong, F. A. *Inorg. Chem.* **2005**, *2005*, 4.
(41) Armstrong, F. A. *Curr. Opin. Chem. Biol.* **2005**, *9*, 110−117.
(42) Sucheta, A.; Cammack, R.; Weiner, J.; Armstrong, F. A. *Biochemistry* **1993**, *32*, 5455−5465.
(43) Bennett, B.; Lemon, B. J.; Peters, J. W. *Biochemistry* **2000**, *39*, 7455−7460.
(44) Patil, D. S.; Czechowski, M. H.; Huynh, B. H.; LeGall, J.; Peck, H. D., Jr.; DerVartanian, D. V. *Biochem. Biophys. Res. Commun.* **1986**, *137*, 1086−1093.

The maximum H_2 oxidation current increases as the pH is raised from 4.3 to 5.9; then it is constant up to pH 8.4 (allowing for continuous slow loss of active enzyme molecules from the electrode). In contrast, the H^+ reduction current decreases steadily as the pH is lowered. It is not possible to determine the absolute electrocatalytic activity of an adsorbed enzyme unless the electroactive coverage is known.[42] This is too low to detect,[45] but taking a value of 1 pmol cm^{-2} as a maximum, we determined lower limits for the turnover frequency, k_{cat}, at 10 °C. These were for H_2 evolution (pH 4.3) 4982 s^{-1}, (pH 5.9) 2210 s^{-1}, and (pH 8.4) 148 s^{-1} and for H_2 oxidation (pH 4.3) 627 s^{-1}, (pH 5.9) 1897 s^{-1}, and (pH 8.4) 1666 s^{-1}. Test experiments at pH 6 showed that increasing the temperature to 25 °C produced an approximate 2-fold increase in H_2 oxidation rate, thereby allowing us to estimate a lower limit of ca. 4000 s^{-1} at 25 °C. Note that these experiments factor out effects of the substrate driving force as the pH is changed: this is because with an electrode, as opposed to a chemical redox partner (such as a dye), the reaction can always be driven in both directions and activity measured as a continuous function of the potential. In vivo, *Dd* hydrogenase is periplasmic and expected to be a H_2 uptake hydrogenase. However, the high H^+ reduction activity of the *Dd* enzyme is not surprising, since it has an active site nearly identical to that of the *Cp* I hydrogenase, which is cytoplasmic, indicating its main biological function is H_2 production.

Inspection of the voltammograms in the region for H_2 oxidation shows that the waveshape is quite complex with suggestion of two current maxima, one close to the transition to inactive enzyme and one at more negative potential (see the voltammogram at pH 5.9, in which this is most clearly evident). However, the relative prominence of either component varied between different sets of experiments, even those carried out at the same pH, and no correlation could be applied to relate, with pH, the electrode potential at which one current maximum merged into the other.[46] Suggestions as to the nature of this waveshape (we would expect the H_2 oxidation region to consist of a flat plateau) will be given later, but at this stage we will focus on the shape and potential dependence of the activity switch-on at more positive potential, which shows a strong correlation with pH and corresponds to the interconversion between inactive (H_{ox}^{inact}) and active (H_{ox}) enzyme. This region of the voltammetric cycle exhibits hysteresis because inactivation occurs more slowly than reactivation (particularly at higher pH), and we address this in section C. (Under conditions of higher temperature (25 °C) and a very slow scan rate (1 mVs^{-1}), it was possible to observe full inactivation and reactivation at pH 4, 6, and 8, and the shapes of the waves in each direction became similar.) Importantly, the switch-on in the scan to negative potential is highly reproducible throughout all our experiments. To quantify the effect of pH on the inactivation/reactivation process (section B), we define the potential E_{switch} as the local minimum in the derivative of the negative sweep of the voltammogram,[14] marked by the circled gray lines in Figure 2. Because reactivation is sufficiently fast, the E_{switch} value for all pH values was independent of the scan rate provided the scan rate was 10 mV s^{-1} or slower.

B. Electron and Proton Transfers in the Active−Inactive Transformation. To determine the number of electrons required in the activation process, we analyzed the sigmoidal increase in current (activity) as the potential was scanned in the negative direction following 100% inactivation at 341 mV. Semilog analysis of the current versus potential data at different pH values yielded straight lines of slopes $2.3RT/nF$, where n is normally the coefficient giving the number of electrons transferred in the process (see the Supporting Information). We obtained the n values 1.2 ± 0.1, 1.3 ± 0.1, and 1.1 ± 0.2 for pH 4, 6, and 9, respectively.[47] The fact that simple, linear plots are observed through the entire pH range (which includes a pK) is consistent with the reductive activation under 1 bar of H_2 being a one-electron reaction rather than two one-electron reactions at similar potentials (which would require exactly compensating similarity in pK values; see below). In terms only of active-site, metal-centered oxidation states, this is interpreted as a transformation from H_{ox}^{inact} (Fe(II)−Fe(II)) to H_{ox} (Fe(I)−Fe(II)).

Figure 3A shows the dependence of E_{switch} values on pH and reveals a pK_{ox} associated with a protonation step linking two oxidized inactive states. A good fit was obtained to eq 2, derived

$$E_{switch} = E_{switch}^{acid} - \frac{2.3RT}{F}\log\left(\frac{a^{H^+} + K_{ox}}{a^{H^+} + K_{red}}\right) \qquad (2)$$

from the Nernst equation under acidic limiting conditions assuming a one-proton, one-electron transfer, and yielded pK_{ox} and E_{switch}^{acid} values of 5.9 and 69 mV, respectively. (In eq 2, R is the gas constant, T is the absolute temperature, F is the Faraday constant, a^{H^+} is the proton activity, and K_{ox} and K_{red} are proton dissociation constants for oxidized and reduced states.) Figure 3B is the corresponding Pourbaix diagram, which depicts the species involved in the coupled electron and proton transfers. Thus, for pH < pK_{ox}, reactivation involves only an electron transfer, whereas, for pH values above pK_{ox}, the reactivation involves transfer of both a proton and an electron. We include a pK_{red} value suggested by the data at high pH (dashed lines in the lower right corner), but we will not discuss this further.

C. Rates of Anaerobic Interconversions between Active and Inactive States. A number of experiments were carried out to compare the rates of interconversions, forward and reverse, between active and inactive states. Our description is

(45) If mass transport to the electrode surface is not a rate-limiting factor and the H_2 concentration greatly exceeds the Michaelis constant, K_M, then it can be stated that $k_{cat} = i_{lim}/FA\Gamma n$, where k_{cat} is the turnover frequency, i_{lim} the maximum current, F the Faraday constant, A the surface area of the electrode (assuming a planar surface), Γ the electroactive coverage, and n the number of electrons transferred per molecule of H_2.

(46) Under H_2 and N_2 the waveshapes did not vary for a single film during the experiment; however, voltammetric cycles recorded during recovery from CO inhibition revealed quite large changes in waveshape as the CO level decreased (early cycles show lower current in the more positive region). This could be due to different active forms having different affinities for CO, which would support the suggestion by Peters and co-workers[43] that H_{ox} forms a more stable complex with CO than does H_{red}.

(47) Since the reactivation process can be viewed as a reduction, $H_{ox}^{inact} + ne^- \rightarrow H_{ox}$, we can express it in terms of the Nernst equation: $E = E^\circ - (2.3RT/nF)\log Q$, where R = molar gas constant, T is the absolute temperature (283 K for all experiments), F is the Faraday constant, and n is the number of electrons involved in the reduction process. We will assume $Q = [H_{ox}]/[H_{ox}^{inact}]$. Positive current, i, is a direct measure of H_2 oxidation activity; thus, the amount of oxidized active enzyme, $[H_{ox}]$, can be stated as $[H_{ox}] \propto i$. The maximum reactivation current, i_{max}, gives a measure of the total amount of enzyme adsorbed on the electrode; thus, the amount of inactive enzyme, $[H_{ox}^{inact}]$, can be stated as $[H_{ox}^{inact}] \propto i_{max} - i$. Therefore, the Nernst equation for the reactivation of the enzyme can be stated as $E = E^\circ - (2.3RT/nF)\log[i/(i_{max} - i)]$. A graph of $\log[(i_{max} - i)/i]$ vs E therefore has a gradient of $nF/2.3RT$.

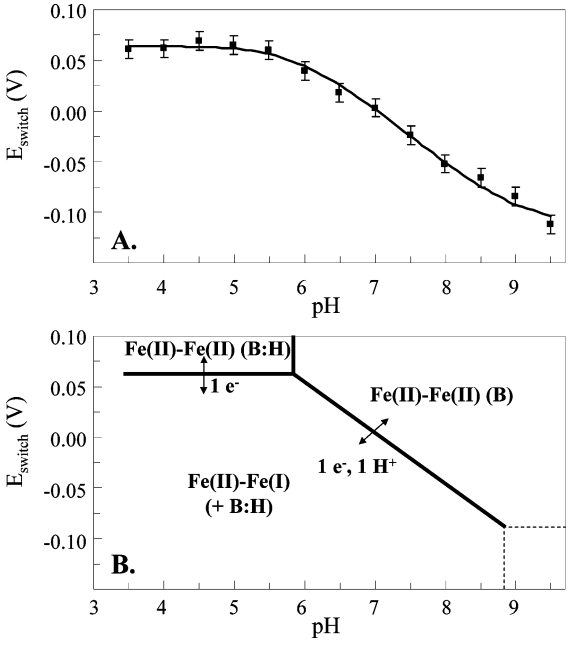

Figure 3. (A) pH dependence of the inactive−active interconversion potential (E_{switch}) for *Dd* [FeFe]-hydrogenase under 1 bar of H_2. Each E_{switch} value was obtained at 10 mV s^{-1}. Other conditions: electrode rotation rate 2500 rpm, 10 °C. Squares depict raw data, and the line shows the fit (according to eq 2) where a one-electron process is assumed. Error bars show the average 95% confidence limit. (B) Pourbaix diagram illustrating a possible interpretation of the data shown in (A). Dashed lines on the lower right indicate the zone for existence of an additional active species suggested by the pH dependence.

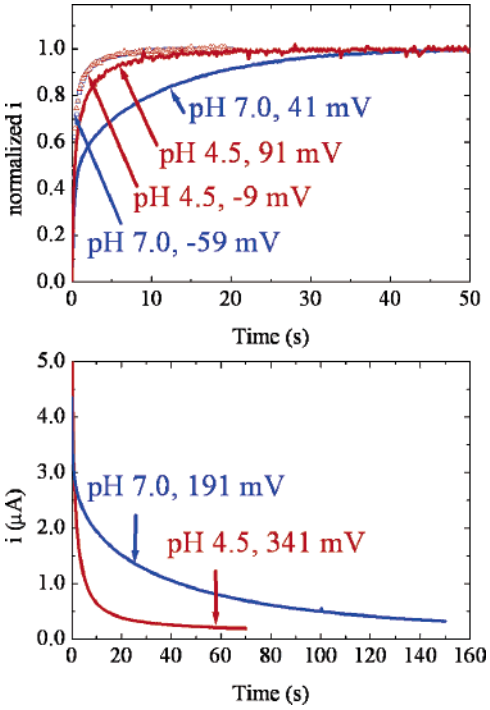

Figure 4. (top) Comparison of the rate of reactivation of *Dd* [FeFe]-hydrogenase at pH 4.5 and 7.0 with high and low thermodynamic driving forces. In both cases, the enzyme was fully inactivated (191 mV for pH 4.5, 341 mV for pH 7.0) before the electrode potential was stepped to a more negative value to induce activation. (bottom) Comparison of the limiting rate of inactivation of *Dd* [FeFe]-hydrogenase at pH 4.5 and 7.0. In both cases, the enzyme was fully activated at −109 mV before the electrode potential was stepped to a positive value. Other conditions: electrode rotation rate 2500 rpm, 10 °C, 1 bar of H_2.

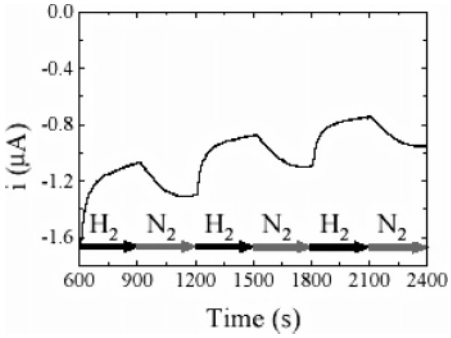

Figure 5. Comparison of the *Dd* [FeFe]-hydrogenase proton reduction activity under 1 bar of H_2 and 1 bar of N_2. The electrode potential was maintained at −459 mV, and the cell was equilibrated with 1 bar of N_2 before the start of the experment. The head gas was changed to H_2 at 10 min and then alternated at 5 min intervals. Other conditions: electrode rotation rate 2500 rpm, pH 6.0, 10 °C.

illuminated by reference to the Pourbaix diagram in Figure 3B, which shows the thermodynamics underlying the reactions. A selection of chronoamperometric traces for the activation direction is shown in Figure 4, top. For pH 4.5, we inactivated the enzyme at 191 mV, and then steps were made to a range of potentials to trigger the activation. These potentials (91, 66, 41, 16, and −9 mV) were chosen to provide a range of driving forces to pull the system across the H_{ox}^{inact}/H_{ox} switch potential (E_{switch}) of the Pourbaix diagram. In all cases, the reaction was fast and the activity reached its maximum value within 10 s, although the rates increased slightly as the potential was made more negative. Our ability to obtain quantitative data was limited by the "dead time" of a few seconds arising from electrode charging effects.[48] A similar experiment was carried out at pH 7.0 in which we started from a potential of 341 mV and stepped to values of 41, 16, −9, −34, and −59 mV, again chosen to provide a similar range of driving force to take the system across the H_{ox}^{inact}/H_{ox} switch potential. As before, the rate of activation increased as the potential became more negative, but even at the most positive potential the enzyme reactivated within 25 s. Thus, activation is fast at both pH 4.5 and pH 7.0.

To measure the slower kinetics of inactivation, a similar strategy was followed except that the starting potential was in the active region (−0.11 V for both pH 4.5 and pH 7.0). Figure 4, bottom, shows traces obtained for potential steps to 191 mV (red line, pH 4.5) and 341 mV (blue line, pH 7.0), i.e., at a high driving force. We analyzed these data only qualitatively as they did not give clean, exponential fits. Inactivation is always slower than activation and is much slower (half-life on the order of a minute) at pH 7.0 at which (from Figure 3) both a electron and a proton must be removed. Therefore, anaerobic inactivation is controlled by a chemical process that involves a proton. This result is significant because the kinetic barrier to inactivation at pH 7 is clearly distinguished from the greater thermodynamic stability of the inactive form at this pH (the Pourbaix diagram shows oxidation is more favorable at alkaline pH).

D. Effect of Inhibitors on Different Oxidation Levels of the Enzyme. Figure 5 shows how H^+ reduction is inhibited by H_2. For this experiment we commenced H^+ reduction at −459 mV under 1 bar of N_2 and then changed the head gas between 1 bar of H_2 and 1 bar of N_2 at 5 min intervals. This resulted in alternate decreases and increases in H^+ reduction current

(48) Hirst, J.; Armstrong, F. A. *Anal. Chem.* **1998**, *70*, 5062−5071.

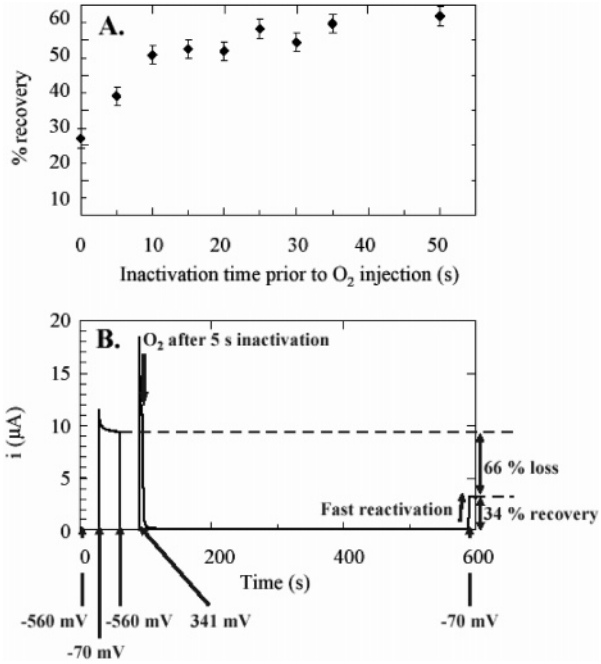

Figure 6. Experiment to observe the O_2 stability of the oxidized, inactive state of *Dd* [FeFe]-hydrogenase. (A) Summary of a series of experiments run as shown in (B). The greater the amount of inactivation preceding O_2 injection (the later the time of injection), the greater the fraction of recovered [FeFe]-hydrogenase activity. (B) Typical current vs time trace: in this example 200 μL of O_2-saturated buffer (corresponding to a final cell concentration of 90 μM) is injected 5 s after the potential is stepped to the inactivating value of 341 mV. Other conditions: electrode rotation rate 2500 rpm, pH 6.0, 10 °C, 1 bar of H_2.

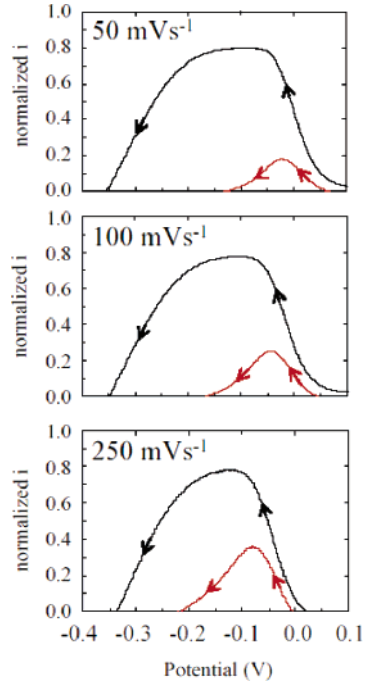

Figure 7. Comparison of the levels of *Dd* [FeFe]-hydrogenase reactivation attained in the presence of CO at different scan rates. The film was first inactivated by poising the electrode potential at 241 mV for 300 s. Arrows show the direction of the scan. Current is normalized with respect to reactivation measured on the previous scan. Black lines indicate the level of reactivation expected if CO is absent; red lines show the reactivation and rapid inhibition observed when 30 μL of CO-saturated solution (final concentration 14 μM) is injected before the scan. Other conditions: rotation rate 2500 rpm, pH 6.0, 10 °C, 1 bar of H_2.

superimposed upon a trend of decreasing current due to enzyme film instability. The effect is quite small, less than 25% attenuation, which is far lower than observed for the [NiFe]-hydrogenase from *Allochromatium vinosum* (*Av*), where inhibition is almost total under 1 bar of H_2 (results not shown).

The experiments shown in Figure 6 were designed to observe the protection afforded by anaerobic oxidation toward the damage due to exposure to O_2. Figure 6A confirms that if the *Dd* [FeFe]-hydrogenase is given sufficient time to inactivate anaerobically prior to O_2 injection, then after O_2 is flushed from the cell the enzyme can be reductively reactivated, showing no loss in activity other than that observed in an O_2-free control.

Each point in Figure 6A was obtained by running experiments as shown in Figure 6B. Thus, the enzyme was activated at low potential (H^+ reduction currents not shown) for 30 s, the catalytic H_2 oxidation activity at −70 mV was measured for 30 s, and then another low-potential, activation step (30 s) was applied. The next stage was a step to 341 mV, at which potential the enzyme inactivates anaerobically, 200 μL of O_2-saturated buffer was injected after 5 s, and the potential was held for 600 s to ensure adequate O_2 flushing time. The final stage was a potential step back to −70 mV to induce rapid reactivation. Comparison of H_2 oxidation currents at the two −70 mV steps showed how much activity has been recovered.

Injection of 0.2 mL of CO-saturated buffer (equivalent to a final concentration of 90 μM CO) at 40 mV caused immediate loss of H_2 oxidation activity. This result is fully consistent with those reported by Thauer and co-workers.[38] Likewise, CO injection at −460 mV caused immediate loss of H^+ reduction activity. Thus, the active states are inhibited by CO, under 1 bar of H_2, irrespective of the direction of catalysis. By contrast, the inactive H_{ox}^{inact} state is unable to bind CO. This is clearly demonstrated in Figure 7, which compares the amount of reactivation observed when H_{ox}^{inact} is exposed to CO and then reactivated at different scan rates.

Data from control experiments, without CO (black line), are included to show the current expected for the reactivated enzyme. In the presence of CO (red line) the activity reaches a maximum and then drops to zero as CO binds. This current transient increases at faster scan rates. This is because the faster the scan rate, the quicker H_{ox}^{inact} is activated to H_{ox} and the shorter the period of time available for CO to bind and block catalysis.

E. Effect of Visible Light on the Rate of Activation of the CO-Inhibited Form. It has been reported that CO ligands bound to hydrogenases are photoactive.[5,23,27,33,34,38,43,44] We therefore investigated how the photoinduced release of exogenous CO might depend upon the electrode potential under catalytic conditions. Results are shown in Figure 8.

The CO-inhibited form was generated by dropwise application of 1 mL of CO-saturated buffer onto the enzyme film, followed by rinsing with deionized water. The potential was then set to −109 mV under 1 bar of H_2 to monitor the oxidation of H_2 as the light was switched on and off at 50 s intervals. This resulted in a clearly defined pattern in which the rate of current increase (directly reporting on the rate of reactivation, i.e., relief of inhibition) was greatly enhanced upon illumination. Then, with the same sample of enzyme, the potential was changed to −459 mV to observe the effect of light when monitoring H^+ reduction. In this case, there was no clear distinction in rates of reactivation between periods of darkness and illumination.[49] The results thus

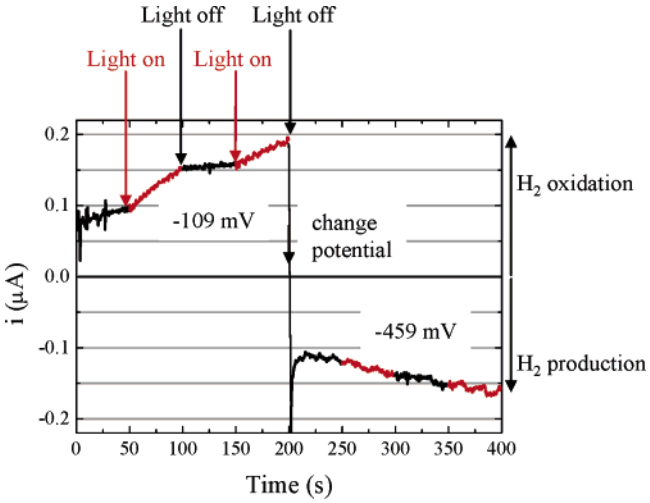

Figure 8. Effect of white light on the recovery of *Dd* [FeFe]-hydrogenase activity after CO inhibition under conditions for H_2 oxidation and H^+ reduction. Black lines indicate light off; red lines indicate light on. The electrode surface was soaked with 1 mL of CO-saturated buffer and then rinsed with water before the experiment was commenced. H_2 oxidation activity (0−200 s) was monitored by holding the electrode potential at −109 mV; H^+ reduction activity (201−400 s) was monitored by holding the electrode potential at −459 mV. Other conditions: electrode rotation rate 2500 rpm, pH 6.0, 10 °C, 1 bar of H_2.

reveal a distinction between two redox states in which a CO is bound, one of which is photolabile, while the other, prevailing at more negative potentials, is photoinert.

Concluding Remarks

This study has merged existing knowledge of the catalytic properties of a well-characterized [FeFe]-hydrogenase with new information resulting from the ability to impose electrochemical control on an enzyme under catalytic conditions.

We have identified three regions of electrode potential that define different levels of catalytic activity and enzyme states. In our hands, the enzyme has high activities for H_2 oxidation and H^+ reduction and undergoes reversible oxidation to an anaerobic "resting" state, identified as H_{ox}^{inact}. In this state, the enzyme is protected against reaction with the irreversible inhibitor O_2 and the reversible inhibitor CO. *D. desulfuricans* is a sulfate-reducing bacterium, therefore the periplasm will be a reducing environment under normal conditions. However, under oxidative stress, conversion of the active site from the catalytically active H_{ox} state to the inactive, O_2-insensitive H_{ox}^{inact} state would provide a mechanism to allow the organism to survive in a dormant form.

We show that, under H_2, H_{ox}^{inact} is formed slowly but activated rapidly at all pH values by addition of one electron (and, above pH 6, a strongly coupled proton). This is in agreement with the Mössbauer results of Pereira et al.[28] and can be reconciled with the observation of Albracht and co-workers, who reported that, in addition to a one-electron reduction, a further two electrons are required at lower potential.[34] The potentiometric titrations showed that oxidative activation at pH 8.0 and 25 °C requires one electron at −92 mV *and* a further two electrons at −301 and −395 mV. In our experiments both an electron *and* H_2 are provided—H_2 being a two-electron reductant and ligand that was not present in the potentiometric titrations. Notwithstanding differences in conditions, the higher value of the "catalytic" potential (approximately −50 mV at pH 8, 10 °C) compared to the first potentiometric value reported by Albracht and co-workers (−92 mV, 25 °C) is not surprising because H_2 binds only once an electron is added (the stabilization of a reduced state by an enhanced ligand binding constant is familiar territory in ligand-coupled electrochemical equilibria). The spontaneity of the reaction with H_2 is also an explanation for the reactivation *n* values exceeding 1.0.

The discovery of two pH-interconvertible forms of H_{ox}^{inact} has particular relevance for crystallography and IR spectroscopy. The p*K* of 5.9 suggests that samples of oxidized inactive *Dd* [FeFe]-hydrogenase prepared at pH values close to 6 might display heterogeneity. The structure of *Cp* I obtained at pH 5.1 by Peters and co-workers is most likely to be the anaerobically oxidized form H_{ox}^{inact},[20,22] and on the basis of our experiments, it should be predominantly in the acid form. J.C.F.-C. obtained the structure of a H_2-reduced form at pH 8.8, corresponding to an active state.[21] The pH dependence that we have determined is classical and shows a strongly coupled proton−electron transfer; thus, it is most likely that the proton binds close to the electron. There are two obvious options: either (1) protonation occurs on the central atom X of the bridging ligand or (2) protonation occurs at a coordinated OH^-/H_2O (as suggested by the *Cp* I crystal structure). Regarding the mechanism of this interconversion, our observations, first of hysteresis and then of differences in the potential-step kinetics for inactivation vs activation, show that the rate of inactivation is limited by a chemical reaction coupled to protonation (thus, it is faster at low pH where a proton is not involved in the equation), whereas activation is always faster.

Our work demonstrates that the CO-inhibited enzyme shows photolability when measured for its ability as a H_2 oxidizer, but not when the enzyme acts as a H^+ reducer (when CO release occurs at a steady rate regardless of illumination). This statement needs to be refined because the apparent dependence on the catalytic direction that we see is simply a reflection of the potentials applied in each case, −109 and −459 mV, respectively, and we interpret this result as demonstrating the existence of (at least) two CO-bound forms, with the state that prevails at −109 mV (but not at −459 mV) displaying photolability. The general observation of photoactivation is in good agreement with results of experiments that address enzyme activity under H_2 at room temperature, for example, as reported by Thauer and co-workers.[38] Interestingly, in a recent paper, it was reported that "the CO-inhibited active form (H_{ox}-CO state) (is) stable in light"; however, that conclusion was based upon spectroscopic experiments that did not allow for reaction with H_2,[34] and it is likely that CO is not released until it is displaced by H_2. Clearly, more information is needed, and the kinetic and thermodynamic influences, as well as the photochemistry, must be resolved. Our own observations, combining turnover measurements with potential control, suggest new experiments in which the rates of activation of CO-inhibited enzyme are examined as functions of potential, wavelength, and light intensity.

(49) Control experiments revealed that, in the presence of light, the rate of film loss decreases at both potentials used in Figure 8. However, this effect is far smaller than the effect of light on recovery of H_2 oxidation activity from CO, with the gradients of film loss changing by no more than a factor of 2.

(50) Zilberman, S.; Stiefel, E. I.; Cohen, M. H.; Car, R. *J. Phys. Chem. B* **2006**, *110*, 7049−7057.

Finally, we note the shape of the voltammograms in the H_2 oxidation region. Of the hydrogenases we have studied so far, only *Av* [NiFe]-hydrogenase shows a simple waveform. Others, including the [NiFe]-hydrogenases from *Ralstonia eutropha* (MBH), *D. vulgaris*, and *Desulfovibrio gigas*, show irregular waveforms with more than one maximum or shoulder.[1] There are several possible reasons for this variability. Inhomogeneity on the electrode is one option. Another is some structural inhomogeneity at the active site that is manifested kinetically but is not obvious from the crystal structure. Structural isomers (forms in which CO and CN ligands have swapped positions[50]) would have to interconvert slowly on our experimental time scale for this to apply. Another proposal is that trace levels of CO interfere because the amount of hydrogenase on the electrode is so small ($\ll$100 fmol) so that even "parts per billion" levels of contaminating CO would cause a visible effect on the waveshape were there to be preferential binding to one particular redox level of the active enzyme, and Peters and co-workers have indeed suggested[43] that CO is bound more tightly to H_{ox}. The possibility that very low background levels of CO might be influential physiologically and be easily evident from the voltammetry suggests another new line of inquiry.

Acknowledgment. F.A.A. and A.P. thank the UK EPSRC and BBSRC (Grants 43/E16711 and BB/D52222X/1) for supporting this work and Dr. Sophie Lamle for her helpful advice. C.C. and J.C.F.-C. thank the CEA and the CNRS for institutional support.

Supporting Information Available: Figure showing the analysis of the number of electrons required to activate *Dd* [FeFe]-hydrogenase. This material is available free of charge via the Internet at http://pubs.acs.org.

JA064425I